

 GLAST LAT TECHNICAL NOTE	Document # LAT-TD-00245-01	Date Effective 16 July 2001
	Prepared by(s) Alexandre Chekhtman J. Eric Grove	Supersedes None
	Subsystem/Office Calorimeter Subsystem	
Document Title CAL Trigger Study		

CHANGE HISTORY LOG

Revision	Effective Date	Description of Changes
1	16 July 2001	Initial Release

Abstract.

A simulation of possible CAL triggers has been done in order to choose CAL HI and CAL LO trigger algorithms and thresholds.

For the CAL HI trigger, a two-stage scheme is proposed, with the first stage done in hardware and the second stage in software. The first stage requires three layers in a row within a tower with at least 1 GeV deposited in at least one crystal in the layer. It provides proton background rejection down to ~15 Hz trigger rate (for primary GCR protons). The second stage uses a cut on the χ^2 from a simple shower direction fit calculated from crystal-ID positions. It decreases the background primary proton rate down to 0.5 Hz, while keeping the efficiency for photons with more than 10 GeV total energy deposition (and in the field of view) above 90 %.

The CAL LO trigger uses a simple OR logic of all crystal-face discriminators with 100 MeV threshold and provides 90% efficiency for 1 GeV photons crossing more than 6 radiation length of CsI.

1 Introduction

The GLAST LAT Calorimeter Subsystem Specification – Level III (document LAT-SS-00018) requires that calorimeter generate a prompt trigger signal with a detection efficiency of >90% for photons that deposit at least 10 GeV in the calorimeter. This trigger is intended to ensure high efficiency for triggering the full LAT for high-energy photons, including those that fail to convert within the tracker.

We searched for simple, fast algorithms that efficiently detect high-energy photons and reject galactic cosmic rays (GCRs). We used glastsim to simulate the passage of photons and protons through the CAL. We used a custom Monte Carlo simulation of GCR pathlengths through calorimeter CsI bars to study energy depositions from the heavier cosmic rays. We used CREME96 to derive the absolute abundances of the GCR species in the GLAST orbit.

We allowed for two-stage algorithms: the first stage could use only simple algorithms easily implemented in hardware logic, while the second stage could use more complicated, calculated quantities applied and manipulated in software. In the first stage, we concentrated on algorithms that could employ no more than a wired-OR of discriminators on the readouts of log faces within a single layer of crystals and simple coincidences among layers. The current calorimeter front-end electronics design will support such discriminators and fast logic.

2 The Backgrounds – Cosmic Rays

The principal source of background capable of depositing >10 GeV in the calorimeter is the GCRs. In LEO, hydrogen and helium comprise more than 99% of the GCRs; thus a discriminator that rejects at least H and He is essential. We can trivially estimate the maximum energy deposition from non-interacting GCR H and He in the CsI bars as follows.

In the GLAST orbit of 28.5 deg inclination, filtering by the geomagnetic field ensures that all of the primary GCRs are relativistic. If we ignore the modest relativistic rise in ionization dE/dx – and the modest corrections for heavy ions – we can assume that all GCRs are minimum ionizing, depositing $1.24 Z^2$ MeV cm^2 / g in CsI. The maximum pathlength in a single $33.3 \times 2.67 \times 1.99$ cm CsI bar is 33.5 cm, which means that He nuclei that do not suffer inelastic nuclear interactions can deposit at most ~ 750 MeV in a single bar. Thus it's likely that any single-log discriminator should be set somewhere above ~ 750 MeV in order to reject the abundant GCRs.

To assess the rate of heavier cosmic rays, we ran CREME96 for the GLAST orbit (28.5 deg inclination, 450 km altitude) at solar minimum and with a quiet geomagnetosphere, which gives the orbit-averaged, isotropized fluxes of all GCR species within the charge range $Z = 1 - 28$. The fluxes are listed in Table 3. The rate of entry of each species into a CsI log is then given by $\pi \Phi_Z \sum_i A_i$, where Φ_Z is the flux of species Z , and $\sum_i A_i$ is the sum of the surface areas of the six faces of a log. If we assume that all GCRs penetrate the calorimeter with negligible slowing-down (which is a good assumption for all but the large-angle, $Z \sim 20$ or heavier cosmic rays), we can estimate the spectrum of their energy depositions by simply scaling the distribution of pathlengths for random, straight tracks through a CsI bar.

We wrote a simple Monte Carlo simulation of the passage of straight tracks through a CsI bar, the output of which is the distribution of pathlengths $P(x)$ for cosmic rays. The distribution of energy depositions of species Z is then given by

$$N_Z(E) = \left(\pi \Phi_Z \sum_i A_i \right) Z^2 \left(\frac{dE}{dx} \right)_{MIP} P(x)$$

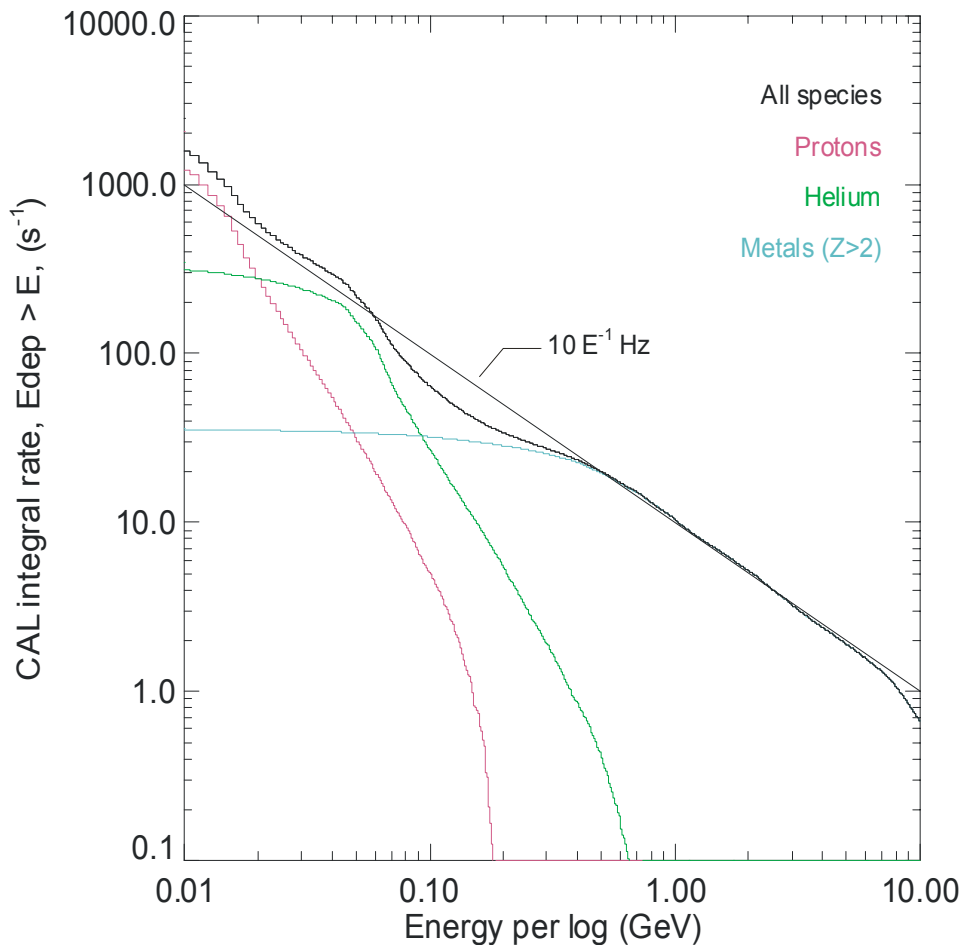


Figure 1. Integral rate in the full LAT CAL of energy depositions greater than E in a single log from GCRs. Note that only ionization energy loss is considered; inelastic nuclear interactions are ignored

where $(dE/dx)_{MIP} = 5.61 \text{ MeV / cm}$ is the rate of ionization energy loss for a minimum-ionizing particle in CsI, $P(x)$ is the pathlength distribution in units of cm, and $\pi \Phi_Z \Sigma_i A_i$ is the rate of entry of species Z into a CsI log.

2.1 Backgrounds we ignored

We ignored albedo protons – both splash albedo and re-entrant albedo – because the flux above several hundred MeV is small compared to the primary protons.

We ignored trapped protons because the LAT will not be operating with the SAA.

We ignored the anomalous cosmic rays because their flux is small, particularly above several GeV/n.

We ignored electrons – both primary GCR electrons and albedo – because the flux above 10 GeV is small. The number spectrum of primary electrons (at Palestine, but that's close enough for our purpose) is approximately given by $0.7 (E_{\text{GeV}} + 1)^{-3.3} \text{ m}^{-2} \text{ s}^{-1} \text{ sr}^{-1} \text{ GeV}^{-1}$ (Komori 1999), so the integral rate above 10 GeV into the $22 \text{ m}^2 \text{ sr}$ geometry factor of the CAL is $< 0.1 \text{ Hz}$.

We ignored photon albedo from the Earth's atmosphere. To the extent that such photons generate valid CAL-HI triggers, they must be filtered on board or allowed to fill telemetry.

3 The Sources – Photons

A 10 GeV photon will typically deposit $\sim 6 \text{ GeV}$ in the $\sim 8.5 \text{ RL}$ calorimeter at $\sim 30 \text{ deg}$ zenith angle. Photons of incident energy $\sim 20 \text{ GeV}$ are more typical of those that deposit at least the requisite 10 GeV for CAL-HI triggers. We therefore chose to simulate 20 GeV photons incident on the LAT with uniform angular distribution in the region $0 < \theta < 70^\circ$, $0 < \phi < 360^\circ$, and we studied the pattern of energy depositions with the CsI crystals for those photons that deposited at least 10 GeV in the CAL. To verify the trigger efficiency at higher energies we also simulated 30 GeV photons with the same angular distribution.

Simulation was done using the `gsmw v1r1` application, and events were written to the IRF file. This file then was read by CalRecon test program, which was modified to provide the output ascii file containing response and identification for every hit log as well as Monte Carlo truth information on the initial particle energy and direction. This ascii file was analyzed with IDL.

Flux of incident particles was generated uniformly over 6 m^2 surface transversal to the particle momentum. Studied samples contained 10000 events for both 20 GeV and 30 GeV photons and 50000 events for CHIME spectrum protons.

4 Trigger scheme selection.

The distribution of total energy deposition in the calorimeter for 20 GeV photons and CHIME protons is shown on fig. 2.

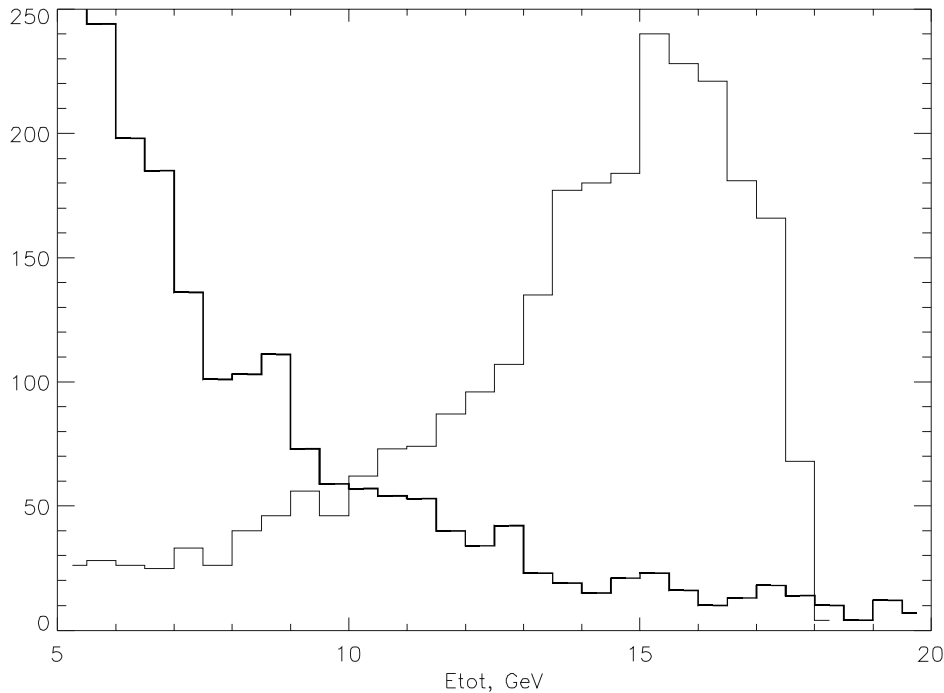


Figure 2. Energy deposition in the calorimeter: for 20 GeV photons - solid line, for CHIME protons - bold line.

The trigger scheme should provide the best possible rejection of protons while keeping the efficiency for photons better than 90% (for $E_{\text{tot}} > 10$ GeV). We propose a 2-level trigger scheme: 1st (hardware) stage uses only logic outputs from discriminators in each channel, combined into OR signals for each layer within a tower; 2nd (software) stage can use all digitized information from the calorimeter.

The choice of discriminator threshold is illustrated on Fig.3, where the maximum energy deposition for the layer that contains the peak of the shower is shown in (b), the layer before the peak in (a), and the layer after the peak in (c). The threshold around 1 GeV satisfies the efficiency requirement for photons, if we use the coincidence of subsequent layers.

We considered several possibilities for level 1 trigger logic, requiring coincidence of OR signal from 1,2,3 or 4 layers in a tower. The trigger logic was simulated by an IDL program, reading an ASCII file produced by the detector simulation and calculating the efficiency of all possible trigger logics as a function of discriminator threshold.

If we suppose that acceptable inefficiency for photons is equally shared between level 1 and software trigger stages, then both are equal to 95%. For every coincidence we considered, we determined the discriminator threshold that satisfies this condition and measured the proton rejection efficiency. The thresholds and efficiencies are given in Table 1.

Table 1. Proton rejection rates for 95% photon efficiency.

Trigger logic	Discriminator threshold, GeV	Proton rejection
Any layer	2.07	0.026
2 layers in a row	1.6	0.008
3 layers in a row	1.1	0.006
4 layers in a row	0.43	0.021

We've chosen "3 in a row" logic because it has the best proton rejection.

Total rate of protons crossing the calorimeter could be determined from proton flux $\Phi=107.7 \text{ m}^{-2} \text{ s}^{-1} \text{ sr}^{-1}$ given in table 1 and the surface S of the calorimeter (box with sizes $1.7*1.7*0.17 \text{ m}^3$): $S=2*1.7*1.7+4*1.7*0.17=6.9 \text{ m}^2$, which gives rate equal to $\pi S\Phi = \pi * 107.7 * 6.9 = 2.35 \text{ kHz}$. So, after rejection with 3 in a row level 1 trigger logic we will get proton rate of $0.006*2.35\text{kHz} = 14 \text{ Hz}$, ignoring albedo.

For further rejection the software trigger will be used where we'll have access to all calorimeter information and a possibility to use more efficient cuts:

We can calculate total energy deposition and apply directly the cut $E_{tot} < 10 \text{ GeV}$ to all events.

Then, we can apply again 3-in-a-row logic, but with discriminator threshold depending linearly with E_{tot} – this will permit to reject better the protons with high energy depositions. For the following analysis we used discriminator threshold $l_{ld} = 1.0 \text{ GeV}$ for $E_{tot} < 15 \text{ GeV}$ and $l_{ld} = 1.0 + (E_{tot} - 15) * 0.1 \text{ GeV}$ for higher energy depositions.

Finally, we can make a fit of shower direction using the information on layer, column and energy in logs hit by the event, and use χ^2 of this fit in x and y directions as the selection criteria. The direction fit is explained below in more detail.

To fit shower direction in the xz plane, we use the 4 layers where logs are oriented along the y axis, and so log number gives the x coordinate and layer number the z coordinate. Every hit log is considered as a point with the weight equal to energy deposited in this log. These points are fitted with linear function $x = A_x * z + B_x$. Parameters A_x and B_x are determined from minimization of the function $\sigma_x^2 = \sum_i (A_x z_i + B_x - x_i)^2 \cdot E_i \rightarrow \min$.

On Fig.4 σ_x^2 is shown as a function of parameter A_x (slope of the line). The quadratic increase with A_x is due to contribution of longitudinal shower spread for non-vertical showers. To account for this, we will use the corrected parameter $\sigma_{x,cor}^2 = \sigma_x^2 - 0.35 * A_x^2$. For this parameter, the average value for photons doesn't depend on A_x and protons are more efficiently rejected. The same correction is applied for the fit in y direction.

A scatter plot of $\sigma_{x,cor}^2$ vs $\sigma_{y,cor}^2$ for 20 GeV photons is shown on Fig. 5. The boxed region shows cuts $\sigma_{x,cor}^2 < 0.4$ and $\sigma_{y,cor}^2 < 0.4$ used for background rejection. Most photons satisfy these conditions. The same distribution for protons is shown on Fig. 6.

Only 4 protons from 50000 simulated events satisfy the selection criteria. To convert this number to the proton rate we take into account that the number of protons giving non-zero energy deposition in the calorimeter is 23539, and this corresponds to 2.35 kHz of total primary GCR proton rate, calculated above. So 4 protons corresponds to 0.4 Hz of residual proton rate after the software CAL HI trigger stage. The number of 20 GeV photons satisfying the selection criteria is 2056, while the number of photons with energy deposition in the calorimeter $E_{tot} > 10 \text{ GeV}$ is equal to 2283, so the efficiency for 20 GeV photons is 90.1%.

Analysis of 30 GeV photons sample shows that the peak values of the $\sigma_{x,cor}$ and $\sigma_{y,cor}$ distributions are bigger than for 20 GeV photons, so to keep the photon efficiency independent of energy we should make this cut energy dependent:

$$\sigma_{x,cor}^2 < \sigma_{cut}^2, \quad \sigma_{y,cor}^2 < \sigma_{cut}^2, \quad \text{where } \sigma_{cut}^2 = 0.3 + 0.01 * E_{tot} \text{ (GeV)}.$$

For this selection we got the photon efficiency almost independent on energy: 91.2% for 20 GeV and 91.0% for 30 GeV photons, while the rejection factor for protons is $2.1 \cdot 10^{-4}$ and corresponding proton rate is 0.5 Hz.

In Table 2 the cuts used at software stage of CAL HI trigger are listed.

Table 2: CAL-HI trigger software cuts

Etot > 10 GeV
If (Etot > 15 GeV) LLD = 1.0 + (Etot - 15) * 0.1 else LLD = 1.0
3 layers in a row having each at least 1 log end with E > LLD
$\sigma_{x,cor}^2 < \sigma_{cut}^2$, $\sigma_{y,cor}^2 < \sigma_{cut}^2$, where $\sigma_{cut}^2 = 0.3 + 0.01 \times E_{tot} (GeV)$.

5 CAL LO trigger threshold.

The Calorimeter LOW trigger threshold is defined by the requirement to have more than 90% efficiency for 1 GeV photons with angle inside field of view of the instrument, which crossed more than 6 radiation length of CsI. Such photons should deposit about half of their energy (500 MeV) in the calorimeter. For our study we simulated 1 GeV photons using the same software as for CAL HI trigger study described above. We selected events with total energy deposition $E_{tot} > 300$ MeV. On fig. 7 the distribution for the maximum energy deposition in a log is shown. Total number of events in the histogram is 1926, and the selection $E_{max} > 100$ MeV is satisfied by 1796 events, so efficiency for this CAL LO trigger threshold is equal to $1796/1926 = 93.2\%$. So, this threshold fits the requirement.

The CAL LO trigger is therefore a logical OR of all log faces within each tower on a 100 MeV discriminator.

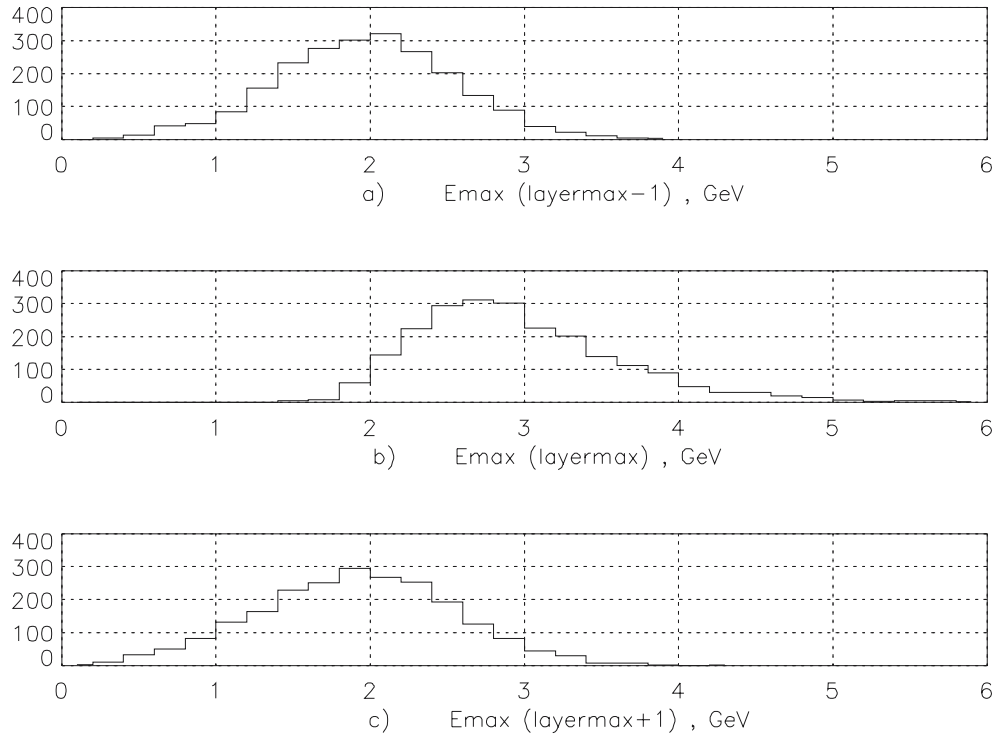


Figure 3. Distribution of maximum response in a layer for 20 GeV photons with total energy deposition >10 GeV: (b) - in the peak of the shower, (a) - in previous layer, (c) - in the next layer.

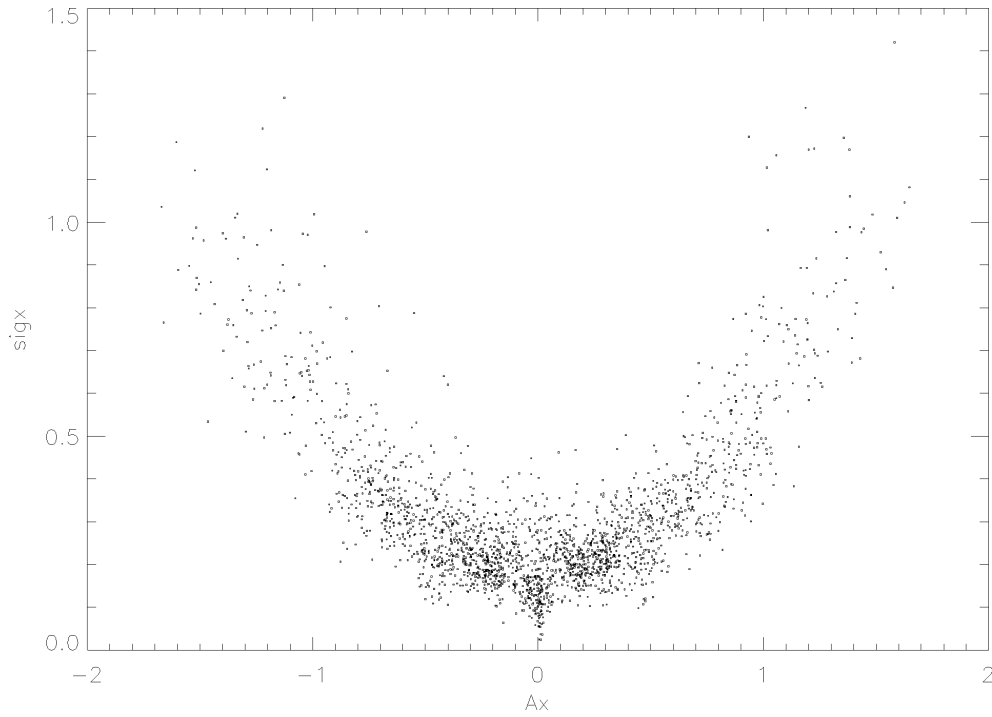


Figure 4. Chi-squared for x-fit as a function of the slope of fitted line.

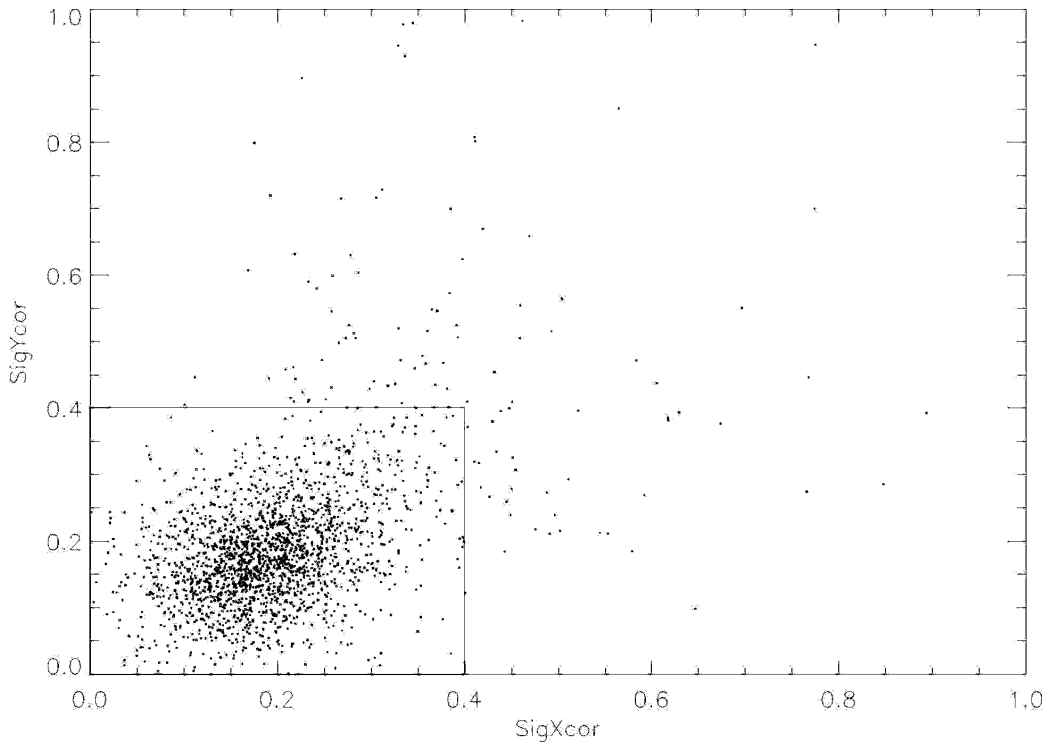
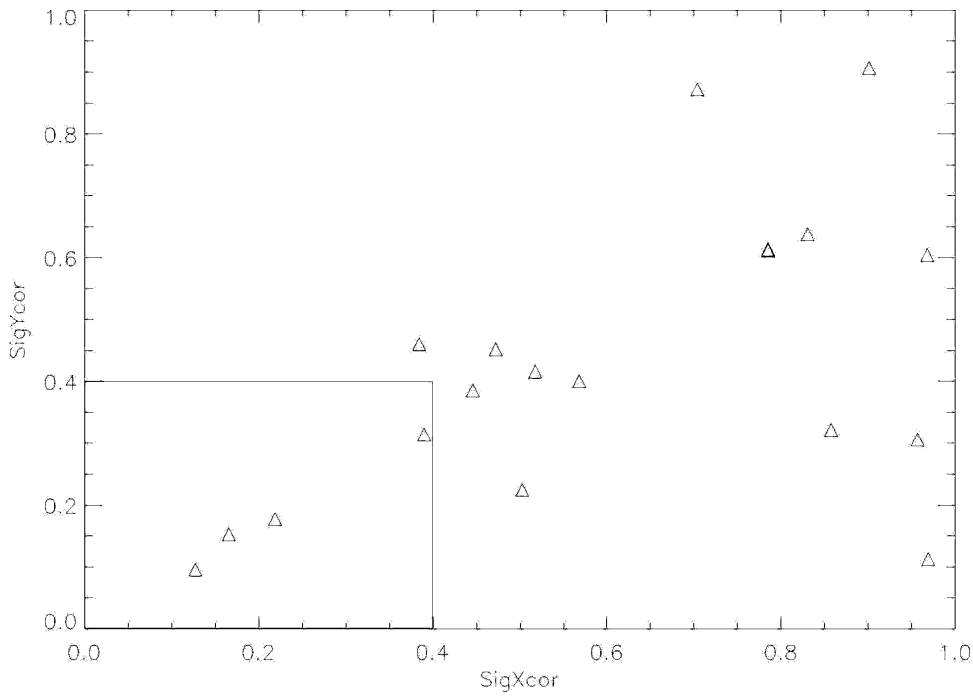
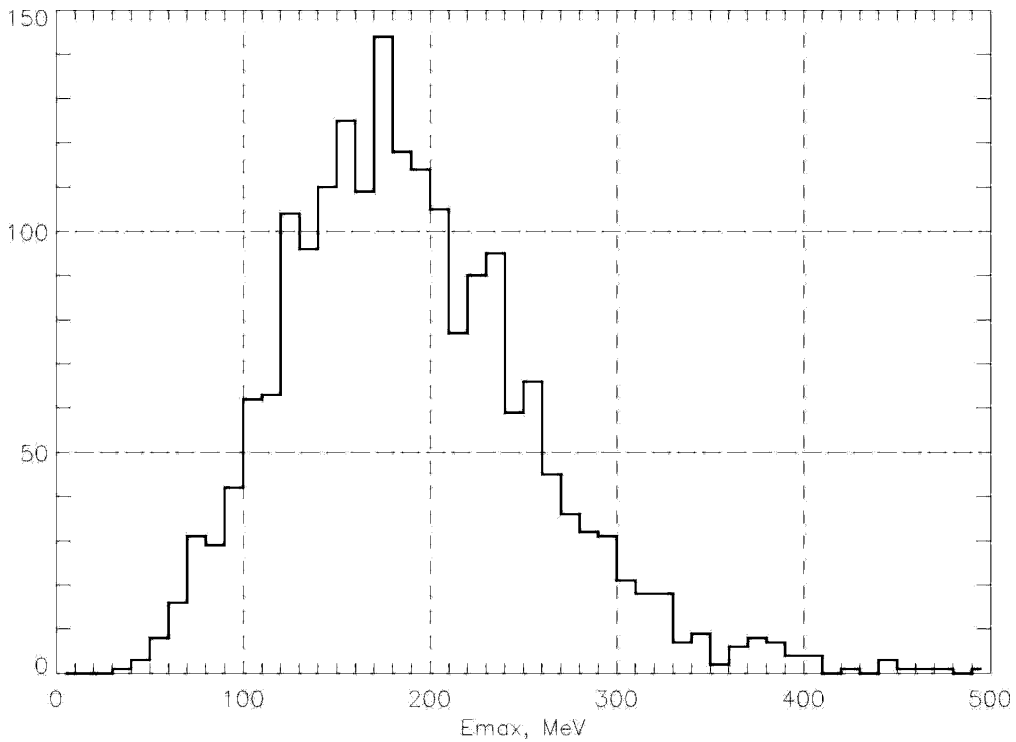


Figure 5. Corrected sig_x and sig_y distribution for 20 GeV photons. Rectangular shows applied cuts.



6

Figure 6. Corrected sigx vs sigy distribution for protons. Rectangular shows applied cuts.



7

Figure 7. Energy in a log with maximum energy deposition for 1 GeV photons with $E_{\text{tot}} > 300$ MeV.

8 Appendix 1: GCR fluxes in the GLAST orbit

The following table lists the flux of galactic cosmic rays in a 28.5 deg inclination, 450 km altitude orbit at solar minimum and with a quiet geomagnetosphere, as derived by CREME96.

Z	Flux ($\text{m}^{-2} \text{s}^{-1} \text{sr}^{-1}$)
1	107.7
2	18.2
3	0.100
4	0.054
5	0.134
6	0.499
7	0.121
8	0.500
9	0.0095
10	0.078
11	0.014
12	0.107
13	0.018
14	0.082
15	0.0030
16	0.016
17	0.0031
18	0.0077
19	0.0047
20	0.014
21	0.0024
22	0.0075
23	0.0039
24	0.0083
25	0.0062
26	0.072
27	0.0004
28	0.0035

Table 3: Integral GCR fluxes in GLAST orbit